Mitigation of Nominal Signal Deformations on Dual-Frequency WAAS Position Errors

Gabriel Wong, Yu-Hsuan Chen, R. Eric Phelts, Todd Walter, Per Enge,
Stanford University

BIOGRAPHY

Gabriel is an R&D engineer at the DSO National Laboratories in Singapore. He received his B.S. in Electrical Engineering from the University of California at Berkeley, and his M.S. and Ph.D. in Electrical Engineering from Stanford University. His research interests include high-integrity navigation and embedded GNSS receivers.

Yu-Hsuan Chen is a research associate at the Stanford GPS Laboratory. He received his Ph.D. in electrical engineering from National Cheng Kung University, Taiwan. His research interests include real-time GNSS software receiver, antenna array processing and APNT.

R. Eric Phelts, Ph.D., is a research engineer in the Department of Aeronautics and Astronautics at Stanford University. He received his B.S. in Mechanical Engineering from Georgia Institute of Technology in 1995, and his M.S. and Ph.D. in Mechanical Engineering from Stanford University in 1997 and 2001, respectively. His research involves signal monitoring techniques and analysis for SBAS, GBAS, and ARAIM.

Todd Walter, Ph.D., is a senior research engineer in the Department of Aeronautics and Astronautics at Stanford University. Dr. Walter received his Ph.D. from Stanford and is currently working on modernization of the Wide Area Augmentation System (WAAS) and defining future architectures to provide aircraft guidance. Key contributions include early prototype development proving the feasibility of WAAS, significant contribution to the WAAS MOPS, design of ionospheric algorithms for WAAS, and development of dual frequency algorithms for SBAS. He is a fellow and past president of the Institute of Navigation.

Per Enge, Ph.D., is a professor of aeronautics and astronautics at Stanford University, where he is the Kleiner-Perkins Professor in the School of Engineering. He directs the GNSS Research Laboratory, which develops satellite navigation systems. He has been involved in the development of the Federal Aviation Administration's GPS Wide Area Augmentation System (WAAS) and Local Area Augmentation System (LAAS). For this work, Enge has received the Kepler, Thurlow, and Burka awards from the Institute of Navigation (ION). He received his Ph.D. from the University of Illinois. He is a member of the National Academy of Engineering and a Fellow of the IEEE and the ION.

ABSTRACT

Global Navigation Satellite Systems (GNSS) are used in a wide variety of applications, some critical, many essential. They are steadily being improved with the addition of new constellations, new frequencies, and new signals. Future multi-frequency GNSS will eliminate one of the largest error sources (ionospheric delays) and promises even better performance.

Unfortunately, the new frequencies and signals will have small but unavoidable biases relative to one another. These nominal satellite signal deformations – deviations of broadcast satellite signals from ideal – result in tracking errors, range biases, and position errors in GPS receivers. The impact of these biases increases as other error sources are eliminated. Left unquantified and unmitigated, future performance may be limited by these biases. Thus it is imperative to measure, characterize, and mitigate them.

An effective "measure-and-verify" measurement technique for signal deformation biases was previously demonstrated by the author and collaborators for L1-frequency signals [**15**]. This two-stage process produced highly-consistent measurements, thus rendering signal deformation biases observable and measurable. This measurement method is applied to obtain signal deformation bias measurements for 3 of the recent Block IIF dual-frequency L1/L5 satellites.

These dual-frequency measurements are subsequently used to validate past projections of dual-frequency L1/L5 biases from single-frequency L1-only biases. In turn, this allows accurate estimations of expected and worst case

position errors for dual-frequency L1/L5 positioning in the presence of unmitigated signal deformation biases.

Finally, using the "measure-and-verify" technique, a proposed strategy is demonstrated to be highly effective: narrowing the space of allowed user-receiver correlator spacings. Use of this strategy mitigates the signal deformation biases and resultant position errors, allowing dual-frequency users to reap the performance benefits of ionospheric error removal without significant limitations caused by signal deformation biases.

INTRODUCTION

Wide Area Augmentation System (WAAS) was developed by the Federal Aviation Administration (FAA) for civil aviation users. WAAS targets to meet the accuracy, integrity, and continuity requirements of en route and terminal phases of flight, and non-precision and near-Category I precision approaches. WAAS is designed to be available all the time, to user receivers at all locations, for all classes of aircraft [**16**].

To meet the stringent safety requirements, WAAS is required to provide highly-accurate position estimates to users (4 m errors at 95% confidence; 10-meter errors at 99.99999% confidence) with high integrity, i.e., to guarantee that users have only an extremely small chance (1 in 10,000,000) of experiencing hazardously large positioning errors. WAAS is also required to provide timely warnings to users when the GPS/ WAAS system is unusable due to faults, system errors, or other effects. While meeting these integrity requirements, WAAS is also expected to maintain 99.999% availability.

To meet these stringent requirements, various errors must be mitigated effectively. These include errors at the receiver such as multipath and receiver noise, propagation errors such as tropospheric and ionospheric delays, and signal-in-space errors such as clock, ephemeris, and the lesser known signal deformation biases.

Signal deformations are deviations of GNSS satellite signals from ideal, and they originate from the satellite's signal generation hardware. Under nominal, everyday operating conditions, these signal deformations are different for individual satellites [**12**], as shown in Fig 1, and result in pseudorange and position errors [**13, 14, 15**].

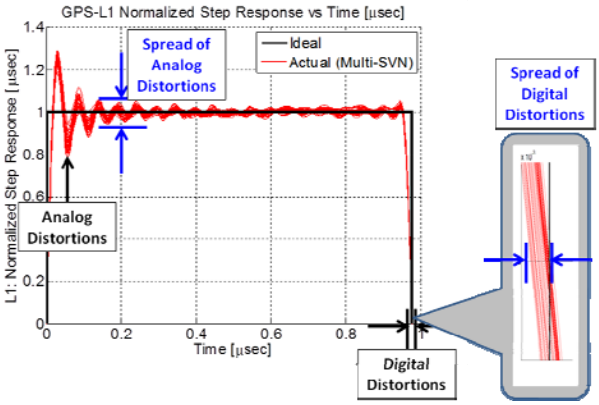

Figure 1. Nominal *Analog and Digital Distortions as measured for different GPS satellites. Data collected with SRI 46m-Dish: Aug 2008, Jul 2009, Aug 2010.*

In WAAS, the error bound for the ionosphere is dominant in single-frequency positioning (Figure 1) [**15**]. Thus there are significant integrity benefits to removing the ionospheric errors.

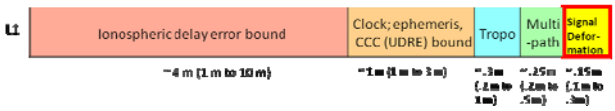

Figure 2. *Nominal Single-frequency WAAS error bounds. The ionospheric error bound is dominant while the signal deformation bias error bound is insignificant in comparison.*

One of the most widely-used and effective ways is through the use of dual-frequency positioning. However, in the process of removing the ionospheric errors, the previously insignificant error bound for signal deformation biases (Figure 1) will be amplified. That error bound will become a significant component of the new, smaller overall error bounds (Figure 2).

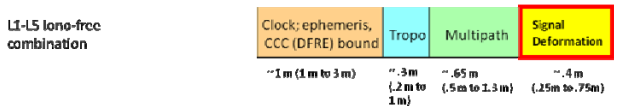

Figure 3. *Nominal Dual-frequency WAAS error bounds including* ***unmitigated*** *signal deformation biases. Ionospheric error removal scales the signal deformation biases, and these now make up a significant component of the new, smaller error bounds.*

The goal is to mitigate these biases effectively, thus enabling WAAS users to benefit from dual-frequency positioning without being adversely impacted by signal deformation biases (Figure 4).

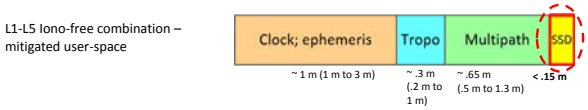

Figure 4. *Nominal Dual-frequency WAAS error bounds including* ***mitigated*** *signal deformation biases.*

Consequently, it is essential to develop measurement techniques to accurately characterize the biases as well as verify the effectiveness of mitigation methods. This will facilitate meaningful estimates of their impact on SBAS positioning performance.

Previous measurement techniques for signal deformations have suffered from the following limitations:

1. Insufficient multipath-attenuation:
   Residual multipath from "all-in-view" antennas, even multipath-limiting ones, frequently has a standard deviation as large as or even larger than most of the signal deformation biases.
2. Susceptibility to long-term, time-varying effects such as drifts:
   "One-in-view" antennas may be susceptible to long-term, time-varying effects that can cause the bias measurements to drift. These time-varying effects were exhibited previously by a large 46 m SRI dish [**13**], and will be demonstrated here for a 1.8 m dish on the rooftop of the Stanford GNSS Lab.

The benefits of each method can be leveraged to overcome the individual limitations. The outcome is a highly-effective "measure-and-verify" measurement technique for signal deformation biases [**15**]. A brief introduction to this two-step process follows.

Figure **5** shows the time-varying drifts in the signal deformation bias measurements from a 1.8 m rooftop dish antenna. More importantly, the results also show daily time spans with "low time-varying drifts", between 6 pm – 10 am local time. These are time periods when the biases are relatively constant, especially for narrow correlator spacing differences. By making dish measurements during these time periods, low-multipath signal deformation bias measurements relatively free of time-varying drifts could be obtained.

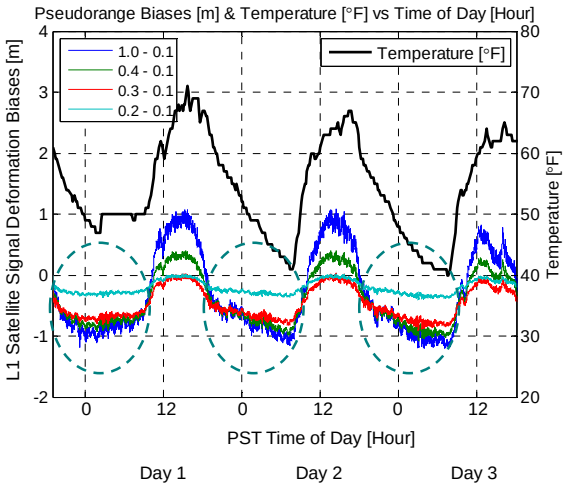

Figure 5. *1.8 m mini-dish antenna on rooftop: Variation of signal deformation biases with temperature and time for different correlator spacing differences, for L1-frequency signals. Reference receiver: 0.1 L1-chip correlator spacing; user receiver: 0.2 L1-chip correlator spacing. The biases are relatively constant between 6 pm – 10 am local time, especially for narrow correlator spacing differences.*

Figure **6** shows 1.8 m low-multipath mini-dish measurements of the single-frequency L1-only signal deformation biases for all available satellites apart from the newly-launched SVN 66/ PRN 27. These daily measurements were made during "low time-varying drift" time periods over almost a year, from July 2012 – Mar 2013. The results shown are for the case of:

- reference receiver: 0.1 L1-chip correlator spacing;
- user receiver: 0.2 L1-chip correlator spacing

As shown in the figure, the standard deviations of the measurements are noticeably smaller in magnitude than the majority of the satellite signal deformation biases. This confirms that the approach provides very good multipath rejection, and accurately measures even the smallest signal deformation biases.

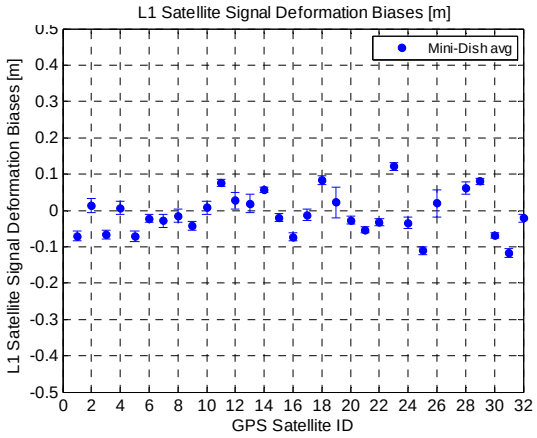

Figure 6. *Signal deformation bias measurements and standard deviations (uncertainty) for individual satellites for the "one-in-view" 1.8 m mini-dish antenna on rooftop. Reference receiver: 0.1 L1-chip correlator spacing; user receiver: 0.2 L1-chip correlator spacing. The average standard deviation ≈ 0.02 m, sufficient to measure even the smallest signal deformation biases.*

To verify that the long-term, time-varying drifts were largely absent from the 1.8 m mini-dish measurements, measurement results from an "all-in-view" choke-ring antenna were used. These measurements were made over two separate one-day periods, at different times of day from those used for the 1.8 m mini-dish measurements.

Figure **7** shows the comparison and remarkable consistency between two sets of results. This suggests that the time-varying biases in the 1.8 m mini-dish measurements are largely absent.

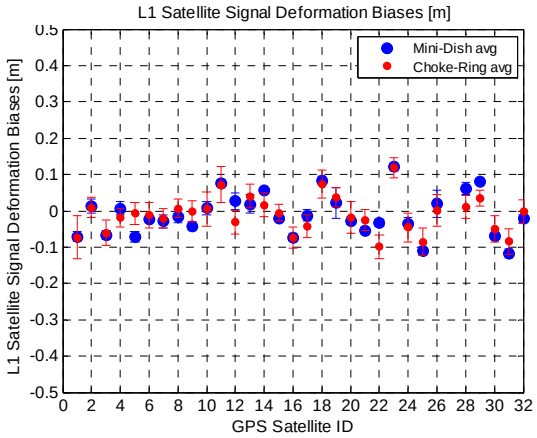

Figure 7. *Signal deformation biases and standard deviations (uncertainty) distributions for individual satellites for "one-in-view" 1.8 m mini-dish antenna and "all-in-view" multipath-limiting antennas on rooftop. Reference receiver: 0.1 chips; User receiver: 0.2 chips. The biases from the two different approaches show remarkable consistency with each other.*

Consequently, this two-step "measure-and-verify" technique renders signal deformation biases observable and measurable with high accuracy and integrity. The presence of these non-zero nominal signal deformation biases is confirmed by previous research findings [**1, 6, 8, 9**].

The remainder of this paper presents the following:

1. Extension of "measure-and-verify" technique to L5-frequency biases: The "measure-and-verify" technique, previously demonstrated for single-frequency L1-only signal deformation biases, is extended to L5-frequency biases in this paper.
2. Validation of projections of dual-frequency L1/L5 biases from single-frequency L1-only biases: Due to the limited number of satellites transmitting dual frequency L1/L5 signals (4 at the time of writing), estimates of SBAS positioning performance are based on projections of dual-frequency L1/L5 biases from single-frequency L1-only biases. Measurements from the "measure-and-verify" technique validate that these projections are reasonable.
3. Computation of vertical position errors from updated measurements: The resultant vertical position errors (95% and worst case) are computed based on the updated measurements, and shown to exhibit significant performance degradation due to the signal deformation biases.
4. Demonstration of effectiveness of proposed mitigation strategy: The "measure-and-verify" technique is used to demonstrate the effectiveness of a proposed mitigation strategy: narrowing the allowed space of user-receiver correlator spacings.

"MEASURE-AND-VERIFY" L5 SIGNAL DEFORMATION BIASES

The "measure-and-verify" measurement technique was applied to measure the signal deformation biases for the GPS satellites which currently transmit signals at the new L5 frequency. These include SVNs 62, 63 and 65 (PRNs 25, 1, 24 respectively) but not SVN 66/ PRN 27, which was launched later than the time of the study.

Figure **8** shows the time traces of single-frequency L5-only signal deformation biases over a day, for the following configuration:

- Reference receiver: 1.0 L5-chip correlator spacing;
- User receiver: 1.4 L5-chip correlator spacing

As can be seen, the biases remain largely constant over the course of 24 hours. Temperature-related time-varying drifts, which were observed for the earlier mini-dish L1-frequency measurements, were absent from the L5-frequency signals over the course of an entire day. As a result, calibration of the mini-dish measurement setup did

not appear necessary and was not employed for these bias measurements.

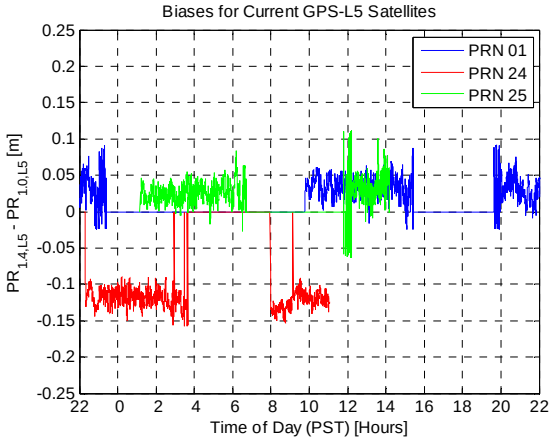

Figure 8. *Time traces of mini-dish L5 signal deformation biases over a day*

Figure **9** shows the signal deformation bias measurements for the three GPS satellites with L5-frequency signals, lined up according to satellites. As before, the configuration was:

- Reference receiver: 1.0 L5-chip correlator spacing;
- User receiver: 1.4 L5-chip correlator spacing

These biases have a maximum magnitude as large as 0.11 m and mean magnitude of 0.06 m.

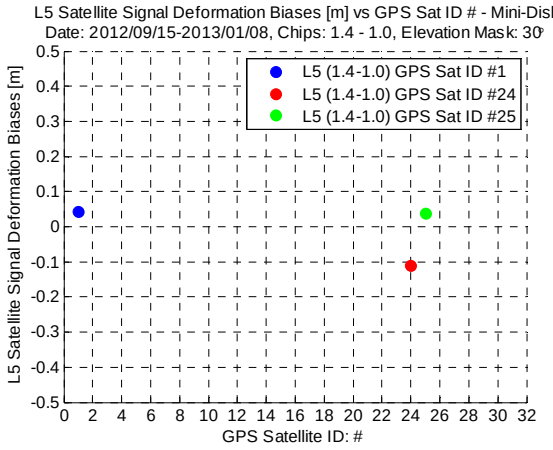

Figure 9. *Signal Deformation Biases for L5, as measured by 1.8 m rooftop mini-dish*

ANALYSIS OF MEASURED DUAL-FREQUENCY BIASES

One of the main concerns with signal deformation biases is their potential amplification when single-frequency pseudoranges of both frequencies (Equations 1 and 2) are used together to eliminate the ionospheric error (Equations 3 and 4).

$$\rho_{L1} = r + c[\delta t_u - \delta t^s] + I_{L1} + T + \varepsilon_{L1} \quad \text{-------- (1)}$$

$$\rho_{L5} = r + c[\delta t_u - \delta t^s] + I_{L5} + T + \varepsilon_{L5} \quad \text{-------- (2)}$$

Where

ρ_{Ln} : Pseudorange at L1-frequency (1.57542) GHz or L5-frequency (1.17645 GHz)
r : True range
c : Speed of light
δt_U : User receiver clock error
δt^S : Satellite clock error
I_{Ln} : Ionospheric error at L1-frequency (1.57542 GHz) or L5-frequency (1.17645 GHz)
T : Tropospheric error (non-dispersive; independent of frequency)
ε_{Ln} : Errors at L1-frequency (1.57542) GHz or L5-frequency (1.17645 GHz), including receiver white noise, multipath and signal deformation biases

$$\rho_{iono-free} = K_{L1} \times \rho_{L1} - K_{L5} \times \rho_{L5} \quad \text{-------- (3)}$$

$$= r + c[\delta t_u - \delta t^s] + T + K_{L1} \times \varepsilon_{L1} - K_{L5} \times \varepsilon_{L5} \quad \text{-------- (4)}$$

Where

K_{Ln} : Scale factor at L1-frequency (1.57542 GHz) or L5-frequency (1.17645 GHz)

The scale factors for L1-frequency and L5-frequency signals, K_{L1} and K_{L5} respectively, are as follows:

$$K_{L1} = \frac{f_{L1}^2}{f_{L1}^2 - f_{L5}^2} \approx 2.26 \quad \text{----------(5)}$$

$$K_{L5} = \frac{f_{L5}^2}{f_{L1}^2 - f_{L5}^2} \approx 1.26 \quad \text{----------(6)}$$

Where

f_{L1} : L1-frequency, 1.57542 GHz
f_{L5} : L5-frequency, 1.17645 GHz

The amplification of the errors in the dual-frequency ionosphere-free pseudorange would be worst in the case when the biases are negatively correlated. Figures 10 and 11 compare these biases for the three aforementioned satellites with both L1- and L5-frequency signals. For these satellites, the biases in the two different frequencies do not appear to show much correlation.

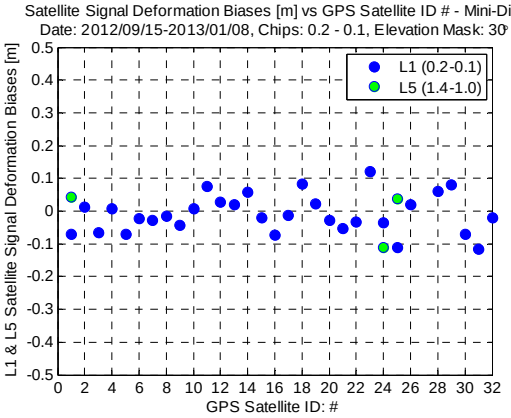

Figure 10. *Signal Deformation Biases for L5, as measured by 1.8 m rooftop mini-dish.*
L1-Frequency receiver configuration:

- *Reference: 0.1 L1-chip correlator spacing;*
- *User: **0.2** L1-chip correlator spacing.*

L5-Frequency receiver configuration:

- *Reference: 1.0 L5-chip correlator spacing;*
- *User: 1.4 L5-chip correlator spacing.*

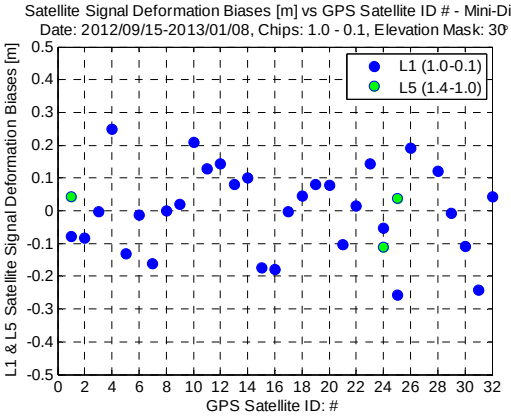

Figure 11. *Signal Deformation Biases for L5, as measured by 1.8 m rooftop mini-dish.*
L1-Frequency:

- *Reference receiver: 0.1 L1-chip correlator spacing;*
- *User receiver: **1.0** L1-chip correlator spacing.*

L5-Frequency:

- *Reference receiver: 1.0 L5-chip correlator spacing;*
- *User receiver: 1.4 L5-chip correlator spacing.*

COMPARISON WITH PREVIOUS SINGLE-FREQUENCY PROJECTIONS

Previously, when GPS satellites transmitting L5-frequency signals were not available, projections of dual-frequency signal deformation biases had to be made from single-frequency biases. Subsequently, as new satellites are launched and become operational, it will be possible to verify that these past projections are reasonable. In this paper, L1-frequency and L5-frequency bias measurements are made for 3 of the dual-frequency satellites and used for such verification.

Table 1 compares the single-frequency L1-only biases from the three satellites broadcasting dual-frequency signals, with the corresponding L1-only biases from the other satellites. As shown in the table, the biases from these three particular satellites do not appear anomalous. However, PRN #25's biases appear to be one of the largest in magnitude.

GPS PRN	L1-Frequency Signal Deformation Biases (m) *User correlator spacing (L1 Chips)*	
	0.2	**1.0**
1	-0.07	-0.08
24	-0.03	-0.05
25	-0.11	-0.26
Others (min)	-0.12	-0.24
Others (max)	0.12	0.25

Table 1. *Comparison of single-frequency L1-only biases from the 3 satellites with dual Frequency signals (PRNs #1, #24, #25) with the biases from the other satellites. The 3 satellites' biases do not appear anomalous. PRNs #25's biases appear to be one of the largest in magnitudes.*

Table 2 shows the computed worst case dual-frequency biases from all possible combinations of the single-frequency L1-only and single-frequency L5-only biases, for different user receiver correlator spacings, for the 3 particular satellites.

From Table 2, we can reach the following conclusions:

1. Among the 3 satellites transmitting dual-frequency L1/L5 signals, PRN25 appears to exhibit the worst-case dual-frequency biases.
2. Measured worst case dual-frequency biases for PRN 25 are approximately 2.6 times that of the single-frequency L1-only biases.
3. There are other satellites whose single-frequency biases are as large as PRN25's. Thus it is a reasonable assumption that worst-case dual-frequency biases for other satellites could be at least as large as that of PRN 25.

GPS PRN	L1-Frequency		L5-Frequency		Dual-Freq. L1/L5 Bias: $K_{L1} \times \text{Bias}_{L1} - K_{L5} \times \text{Bias}_{L5}$
	User corr spcg (L1-chips)	Bias*	User corr spcg (L5-chips)	Bias*	
1	0.2	-0.07	0.6	-0.04	-0.11
24	0.2	-0.03	0.6	0.07	-0.16
25	0.2	-0.11	0.6	-0.04	-0.20
1	0.2	-0.07	1.4	0.04	-0.21
24	0.2	-0.03	1.4	-0.11	0.06
25	0.2	-0.11	1.4	0.04	-0.30
1	1.0	-0.08	0.6	-0.04	-0.13
24	1.0	-0.05	0.6	0.07	-0.20
25	1.0	-0.26	0.6	-0.04	-0.53
1	1.0	-0.08	1.4	0.04	-0.23
24	1.0	-0.05	1.4	-0.11	0.02
25	1.0	-0.26	1.4	0.04	-0.63

Table 2. *Dual Frequency Combination of Unmitigated Satellite Signal Deformation Biases.*
Note: $K_{L1} = 2.26$ and $K_{L5} = 1.26$ (Equations 5 and 6).
**Signal deformation bias*

COMPUTATION PROCEDURES FOR AVAILABILITY, EXPECTED ACCURACIES AND VERTICAL POSITION ERRORS

Following the approaches outlined in [**14**, **15**], the WAAS Vertical Protection Levels, or VPL, are computed [**10**] using the MATLAB Algorithm Availability Simulation Tool (MAAST) developed at Stanford [**7**].

The VPLs are used in the computation of expected nominal accuracy, as well as expected 95% and worst case vertical position errors in the absence and presence of signal deformation biases.

The single-frequency (Equation 7) and dual-frequency variance overbounds (Equation 8) are used in the computation of the VPL. For the i^{th} satellite, these are computed as follows:

$$\sigma^2_{OVERBOUND,L1-ONLY,i} = \sigma^2_{OVERBOUND,UDRE,i} + \sigma^2_{OVERBOUND,UIVE,i} * O^2 + \sigma^2_{OVERBOUND,CNMP,i} + \sigma^2_{OVERBOUND,TROP,i} \quad \text{-------- (7)}$$

where

$\sigma^2_{OVERBOUND,L1-ONLY,i}$: Overall variance overbound for most significant errors, for the single frequency L1-only GPS pseudorange

$\sigma^2_{OVERBOUND,UDRE,i}$: Variance overbound for User Differential Range Errors (UDREs) – satellite clock & ephemeris errors

$\sigma^2_{OVERBOUND,UIVE,i}$: Variance overbound for User Ionospheric Vertical Errors (UIVEs) at each of his ionospheric pierce point locations.

O : Obliquity factor - The increase in path length through the ionosphere that an oblique ray takes relative to a vertical ray [**17**]

$\sigma^2_{OVERBOUND,CNMP,i}$: Variance overbound for airborne receiver & multipath errors

$\sigma^2_{OVERBOUND,TROP,i}$: Variance overbound for tropospheric delay errors

For dual-frequency L1/L5, the variance overbound is:

$$\sigma^2_{OVERBOUNDED,L1/L5,i} = \sigma^2_{OVERBOUNDED,UDRE,i} + \sigma^2_{OVERBOUNDED,CNMP,i} * K^2_{DUAL-FREQ-IONO} + \sigma^2_{OVERBOUNDED,TROP,i} \quad \text{-------- (8)}$$

where

$\sigma^2_{OVERBOUNDED,L1/L5,i}$: Overall variance overbound for most significant errors, for the dual frequency L1/L5 GPS pseudorange

$K_{DUAL-FREQ-IONO}$: Dual-frequency ionosphere-error-removal scale factor.

and $\sigma^2_{OVERBOUNDED,UDRE,i}$, $\sigma^2_{OVERBOUNDED,CNMP,i}$, and $\sigma^2_{OVERBOUNDED,TROP,i}$ are the same quantities as in Equation 7.

Assuming uncorrelated noise and multipath on L1 and L5, the dual-frequency ionosphere-error-removal scale factor, $K_{DUAL-FREQ-IONO}$, is 2.6 (refer Equations 5 and 6):

$$K_{DUAL-FREQ-IONO} = \sqrt{K^2_{L1} + K^2_{L5}} = \sqrt{2.26^2 + 1.26^2} \approx 2.6 \quad \text{-------- (9)}$$

Table 3 shows the different terms used in the VPL equations and the values used. Constant fixed values

across CONUS were used for errors in ionospheric delay, ephemeris and clock.

Error Term in VPL Equations	Description of Error	Overbound Standard Deviation [m]
$\sigma_{OVERBOUND,UDRE}$	Overbounded standard deviation for satellite clock and ephemeris errors. For simplicity, constant fixed values were used over CONUS.	0.84 (Corresponding to 3.29σ value of 3.0)
$\sigma_{OVERBOUND,UIVE}$	Overbounded standard deviation for ionospheric delay errors. For simplicity, constant fixed values were used over CONUS.	1.88 (Corresponding to 3.29σ value of 4.5)
$\sigma_{OVERBOUND,CNMP}$	Overbounded standard deviation for airborne receiver and multipath errors	Nominal overbounded values as calculated by MAAST algorithms
$\sigma_{OVERBOUND,TROP}$	Overbounded standard deviation for tropospheric delay errors	Nominal overbounded values as calculated by MAAST algorithms = 0.12 x Mapping Function

Table 3. *Error Terms used in VPL equations and values used.*

The fault free error variances, also used in the computation of vertical position errors, are computed based on 1.7 billion points of 1 Hz measured data collected at 20 locations within WAAS coverage, following the approach of [**11**].

Finally, the computation of vertical position errors due to signal deformation biases follows the approach outlined in [**14, 15**], and is computed over a day.

EXPECTED AVAILABILITY

Figure 12 shows the availability over CONUS in the case of two unhealthy/ inaccessible satellites for single-frequency L1-only WAAS users. Figure 13 shows the corresponding availability for dual-frequency L1/L5 WAAS users. The figures show the main benefit of dual-frequency positioning: increased availability due to the removal of the differential ionospheric delays, the largest integrity threat.

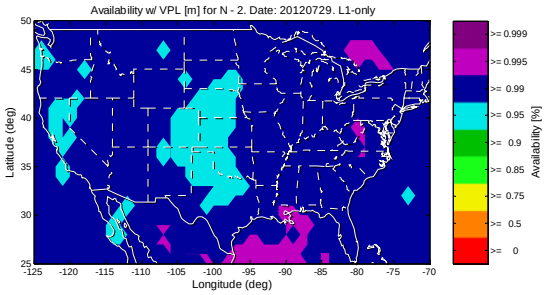

Figure 12. *Availability for the case of two inaccessible satellites for* ***Single*** *Frequency L1-only WAAS Users:*

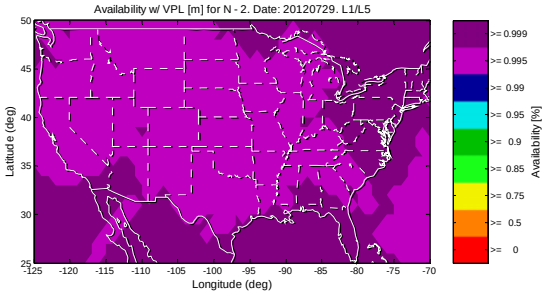

Figure 13. *Availability for the case of two inaccessible satellites for* ***Dual-Frequency*** *L1/L5 WAAS Users:*

Table 4 summarizes these availability results for the cases of different numbers of healthy satellites, from entirely healthy and accessible to 5 inaccessible satellites. For the case of two inaccessible satellites, dual-frequency L1/L5 positioning barely meets the WAAS availability requirement of 99.999% while single-frequency L1-only positioning fails to do so.

Satellite Status	Average Availability [%]	
	Frequency: L1-Only	Frequency: L1/L5
N - 0	100.00%	100.00%
N - 1	99.91%	99.99%
N - 2	99.26%	99.88%
N - 3	97.01%	99.31%
N - 4	91.32%	97.15%
N - 5	80.46%	91.44%

Table 4. *Average Availability for Single Frequency L1-only and Dual Frequency L1/L5 WAAS Users*

EXPECTED ACCURACY IN THE ABSENCE OF SIGNAL DEFORMATION BIASES

Figures 14 and 15 show the nominal accuracy results in the absence of signal deformation biases, for the cases when two satellites are inaccessible. The results shown in these figures can be somewhat counter-intuitive: dual-frequency positioning removes the contribution of differential ionospheric errors, yet results in a worse expected accuracy.

The main reason for this is that under nominal conditions, the ionosphere is quiescent, resulting in small ionospheric delays, limiting the benefit of dual-frequency positioning. On the other hand, multipath errors are present and amplified by dual-frequency positioning, resulting in increased errors, and worse expected accuracy.

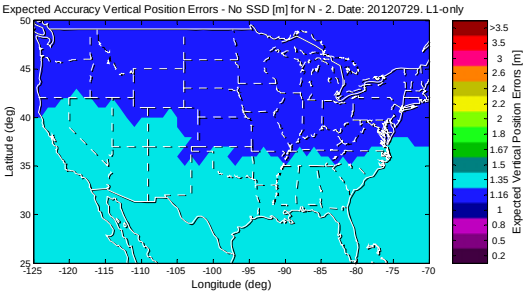

Figure 14. *Nominal Accuracy (95% 2σ) for the case of two inaccessible satellites for Single-Frequency L1-only WAAS Users:*

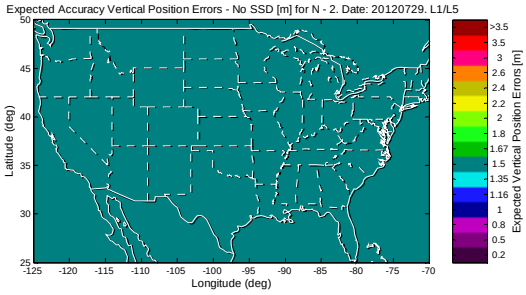

Figure 15. *Nominal Accuracy (95% 2σ) for the case of two inaccessible satellites for Dual-Frequency L1/L5 WAAS Users*

Table 5 summarizes these expected accuracy results for different numbers of healthy satellites, from entirely healthy and accessible to 5 unhealthy/ inaccessible satellites. Slightly degraded expected accuracy is seen for dual-frequency positioning for all six satellite reduction scenarios.

Satellite Status	Average Nominal Accuracy [m]	
	Frequency: L1-Only	Frequency: L1/L5
N - 0	0.99	1.21
N - 1	1.07	1.31
N - 2	1.16	1.43
N - 3	1.27	1.61
N - 4	1.39	1.82
N - 5	1.50	2.06

Table 5. *Average Nominal Accuracy without satellite signal deformation biases for Single L1-only and Dual L1/L5 Frequency WAAS Users*

RESULTANT EXPECTED 95% AVERAGE VERTICAL POSITION ERRORS DUE TO UNMITIGATED SIGNAL DEFORMATION BIASES

Figures 16 and 17 show the nominal accuracy including expected 95% vertical position errors from unmitigated signal deformation biases. These results are shown for single-frequency L1-only and dual-frequency L1/L5 WAAS users, for the case of 2 inaccessible satellites.

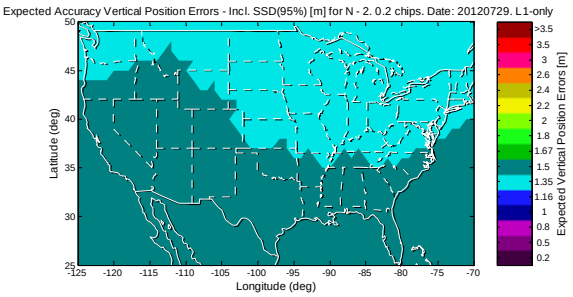

Figure 16. *Nominal Accuracy Including Expected 95% Vertical Position Errors from Unmitigated Signal Deformation Biases [m] for* ***Single Frequency*** *L1-only WAAS Users, for two inaccessible satellites.*
Reference receiver: 0.1 L1-chip correlator spacing; User receiver: 0.2 L1-chip correlator spacing)

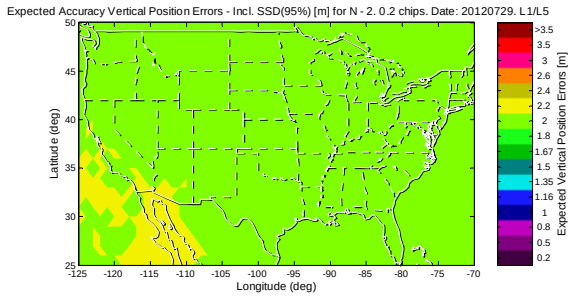

Figure 17. *Nominal Accuracy Including Expected 95% Vertical Position Errors from Unmitigated Satellite Signal Deformation Biases [m] for* ***Dual Frequency*** *L1/L5 WAAS Users, for two inaccessible satellites. Reference receiver: 0.1 L1-chip correlator spacing; User receiver: 0.2 L1-chip correlator spacing*

Tables 6 and 7 summarize these results for single-frequency L1-only and dual-frequency L1/L5 users respectively. Note that the dual-frequency signal deformation biases are projected from single-frequency L1-only satellite signal deformation biases. The figures in parentheses are absolute and percentage increases over the reference results. (The reference results were obtained in the absence of signal deformation biases).

The signal deformation biases contribute an additional 16%-35% of the vertical position errors for single-frequency WAAS positioning, and an additional 31%-76% of the vertical position errors for dual-frequency WAAS positioning. This highlights the importance of mitigation.

Satellite Status	Nominal Accuracy Including **Average Expected 95%** Vertical Position Errors from Unmitigated **Single-Frequency** (L1-only) Signal Deformation Biases [m]		
	User Correlator Spacing [L1-chips]		
	No SSD	Unmitigated	
	0.10	**0.20**	**1.00**
N – 0	0.99	1.15 (+0.16) (+16.2%)	1.29 (+0.30) (+30.3%)
N – 1	1.07	1.24 (+0.17) (+15.9%)	1.41 (+0.34) (+31.8%)
N – 2	1.16	1.36 (+0.20) (+17.2%)	1.55 (+0.39) (+33.6%)
N – 3	1.27	1.49 (+0.22) (+17.3%)	1.71 (+0.44) (+34.6%)
N – 4	1.39	1.63 (+0.24) (+17.3%)	1.87 (+0.48) (+34.5%)
N – 5	1.50	1.76 (+0.26) (+17.3%)	2.02 (+0.52) (+34.7%)

Table 6. *Nominal Accuracy Including Average Expected 95% Vertical Position Errors [m] from Unmitigated Satellite Signal Deformation Biases for* ***Single frequency L1-only*** *WAAS Users. Each row contains results for a different number of inaccessible satellites, from fully accessible to 5 inaccessible.*

Satellite Status	Nominal Accuracy Including **Average Expected 95%** Vertical Position Errors from Unmitigated **Dual Frequency** (L1/L5) Signal Deformation Biases [m]		
	User Correlator Spacing [L1-chips]		
	No SSD	Unmitigated	
	0.10	**0.20**	**1.00**
N – 0	1.21	1.59 (+0.38) (+31.4%)	1.98 (+0.77) (+63.6%)
N – 1	1.31	1.74 (+0.43) (+32.8%)	2.18 (+0.87) (+66.4%)
N – 2	1.43	1.93 (+0.50) (+35.0%)	2.43 (+1.00) (+69.9%)
N – 3	1.61	2.17 (+0.56) (+34.8%)	2.78 (+1.17) (+72.7%)
N – 4	1.82	2.48 (+0.66) (+36.3%)	3.20 (+1.38) (+75.8%)
N – 5	2.06	2.81 (+0.75) (+36.4%)	3.62 (+1.56) (+75.7%)

Table 7. *Nominal Accuracy Including Average Expected 95% Vertical Position Errors [m] from Unmitigated Satellite Signal Deformation Biases for* ***Dual-frequency L1/L5 WAAS Users****. Each row contains results for a different number of inaccessible satellites, from 0 (i.e., all satellites available) to 5 inaccessible.*

RESULTANT WORST CASE VERTICAL POSITION ERRORS DUE TO UNMITIGATED SIGNAL DEFORMATION BIASES

Figures 18 and 19 show the nominal accuracy including worst case vertical position errors from unmitigated signal deformation biases. These results are shown for single-frequency L1-only and dual-frequency L1/L5 WAAS users, for the case of 2 inaccessible satellites.

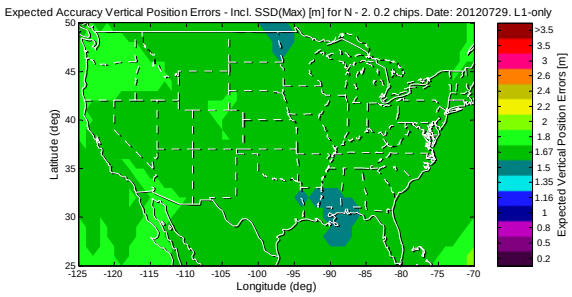

Figure 18. *Nominal Accuracy Including Worst Case Vertical Position Errors from Unmitigated Signal Deformation Biases [m]. Results for Single Frequency L1-only WAAS Users, for two inaccessible satellites. Reference receiver: 0.1 L1-chip correlator spacing; User receiver: 0.2 L1-chip correlator spacing)*

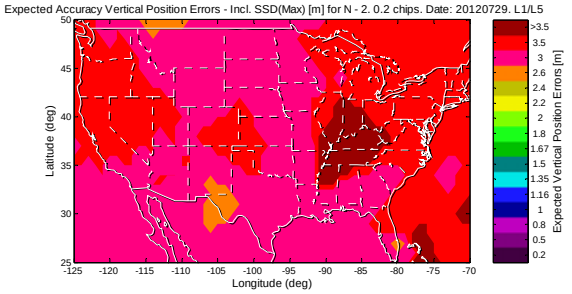

Figure 19. *Nominal Accuracy Including Worst Case Vertical Position Errors from Unmitigated Satellite Signal Deformation Biases [m]. Results for Dual Frequency L1/L5 WAAS Users, for two inaccessible satellites.*
Reference receiver: 0.1 L1-chip correlator spacing; User receiver: 0.2 L1-chip correlator spacing

Tables 8 and 9 summarize these results for single-frequency L1-only and dual-frequency L1/L5 users respectively. Note that the dual-frequency signal deformation biases are projected from single-frequency L1-only satellite signal deformation biases. Also, the figures in parentheses are absolute and percentage increases from the reference results. (The reference results were obtained in the absence of signal deformation biases).

For single-frequency WAAS positioning, worst case vertical position errors from signal deformation biases contribute an additional 21%-91% of error. In dual-frequency WAAS positioning, the increase in error contribution is even more significant: 44%-264%. This highlights the importance of mitigation.

Satellite Status	Nominal Accuracy Including **Worst Case** Vertical Position Errors from Unmitigated **Single Frequency** (L1-only) Signal Deformation Biases [m]		
	User Correlator Spacing [L1-chips]		
	No SSD	Unmitigated	
	0.10	**0.20**	**1.00**
N – 0	0.99	1.20 (+0.21) (+21.2%)	1.41 (+0.42) (+42.4%)
N – 1	1.07	1.39 (+0.32) (+29.9%)	1.78 (+0.71) (+66.4%)
N – 2	1.16	1.62 (+0.46) (+39.7%)	2.18 (+1.02) (+87.9%)
N – 3	1.27	1.81 (+0.54) (+42.5%)	2.43 (+1.16) (+91.3%)
N – 4	1.39	1.96 (+0.57) (+41.0%)	2.59 (+1.20) (+86.3%)
N – 5	1.50	2.10 (+0.60) (+40.0%)	2.72 (+1.22) (+81.3%)

Table 8. *Nominal Accuracy Including Worst Case Vertical Position Errors [m] from Unmitigated Satellite Signal Deformation Biases for* ***Single frequency L1-only*** *WAAS Users. Each row contains results for a different number of inaccessible satellites, from fully available to 5 inaccessible.*

Satellite Status	Nominal Accuracy Including **Worst Case** Vertical Position Errors from Unmitigated **Dual Frequency** (L1/L5) Signal Deformation Biases [m]		
	User Correlator Spacing [L1-chips]		
	No SSD	Unmitigated	
	0.10	**0.20**	**1.00**
N – 0	1.21	1.74 (+0.53) (+43.8%)	2.25 (+1.04) (+86.0%)
N – 1	1.31	2.24 (+0.93) (+71.0%)	3.25 (+1.94) (+148.1%)
N – 2	1.43	3.04 (+1.61) (+112.6%)	5.06 (+3.63) (+253.8%)
N – 3	1.61	3.8 (+2.19) (+136.0%)	5.86 (+4.25) (+264.0%)
N – 4	1.82	4.22 (+2.40) (+131.9%)	6.40 (+4.58) (+251.6%)
N – 5	2.06	4.48 (+2.42) (+117.5%)	6.77 (+4.71) (+228.6%)

Table 9. *Nominal Accuracy Including Worst Case Vertical Position Errors [m] from Unmitigated Satellite Signal Deformation Biases for* ***Dual-frequency L1/L5 WAAS Users****. Each row contains results for a different number of inaccessible satellites, from fully available to 5 inaccessible.*

PROPOSED MITIGATION: NARROW ALLOWED SPACE OF USER RECEIVER CORRELATOR SPACINGS

An effective mitigation strategy is to limit the allowed space of user receiver correlator spacings, to more closely match that of the WAAS reference receivers, as shown in Figures 20 and 21. In fact, this is currently proposed for the next generation of aviation receivers.

In the next section, the "measure-and-verify" measurement technique demonstrates that the proposed mitigation strategy is indeed an effective mitigation strategy against signal deformation biases.

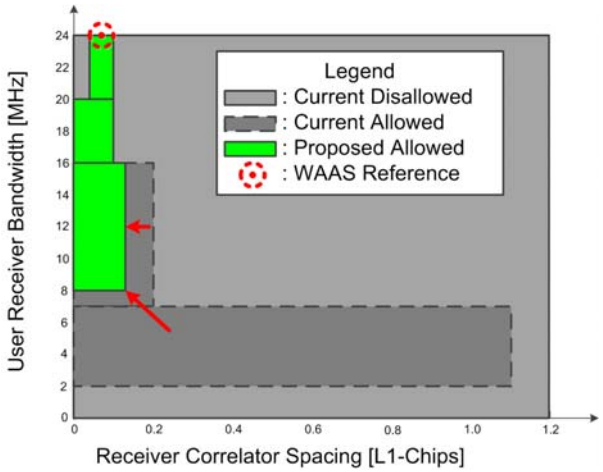

Figure 20. *Narrowing the allowed user receiver correlator spacings for L1.*

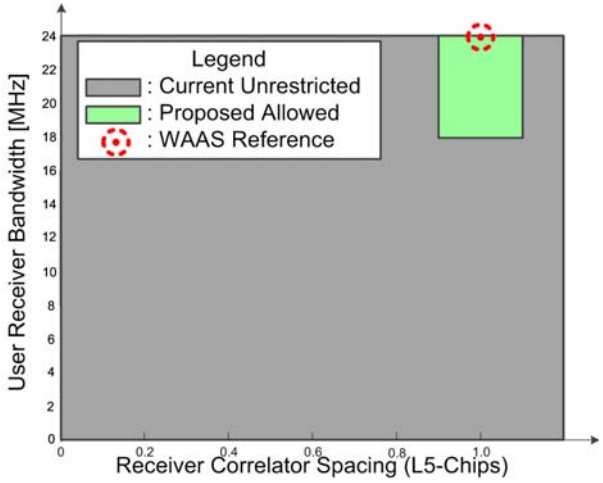

Figure 21. *Narrowing the allowed user receiver correlator spacings for L5.*

USE OF "MEASURE-AND-VERIFY" TO DEMONSTRATE EFFECTIVENESS IN BIAS REDUCTION

In this section, the "measure-and-verify" measurement technique will be used to demonstrate the effectiveness of the mitigation strategy proposed in the previous section: narrowing the allowed space of user receiver correlator spacings.

Fiure 22 shows the signal deformation biases for all satellites transmitting signals on L1-frequency (apart from the newly launched SVN 66/ PRN 27). As the figure demonstrates, narrowing the allowed user receiver correlator spacing from 0.2/1.0 L1-chips to 0.08/0.12 L1-chips significantly reduces the bias magnitudes.

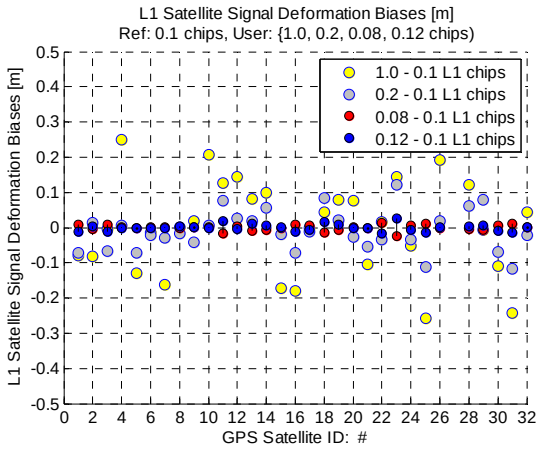

Figure 22. *Comparison of unmitigated and mitigated single-frequency L1-only signal deformation biases for all satellites.*

As summarized in Table 10, narrowing the allowed user receiver correlator spacing reduces the maximum and average bias magnitudes of the single-frequency L1-only signal deformation biases.

Unmitigated maximum bias magnitudes:
- ~0.12 m for 0.2 L1-chips user correlator spacing
- ~0.25 m for 1.0 L1-chips user correlator spacing

Mitigated maximum bias magnitudes:
- ~0.03 m for 0.08-0.12 L1-chips user receiver correlator spacing

Unmitigated average bias magnitudes:
- ~0.05 m for 0.2 L1-chips user correlator spacing
- ~0.11 m for 1.0 L1-chips user correlator spacing

Mitigated maximum bias magnitudes:
- ~0.01 m for 0.08-0.12 L1-chips user receiver correlator spacing

Correlator. Spacing (L1-chips)		Signal Deformation Biases [m]		
Ref.	User	Min	Max	Avg Mag.
0.1	1.0	-0.26	0.25	0.11
0.1	0.2	-0.11	0.12	0.05
0.1	0.08-0.12	-0.02	0.03	0.01

Table 10. *Tabular summary of unmitigated and mitigated single-frequency **L1-only** signal deformation biases*

Similarly, Figure 23 shows the signal deformation biases for the satellites transmitting signals on L5-frequency. (As previously stated, currently there are 4 such satellites; measurement results were collected for the first 3 in this paper, apart from newly-launched SVN 66/ PRN 27). This time, there is reduction in bias magnitudes, but not as significantly as in the L1-frequency case.

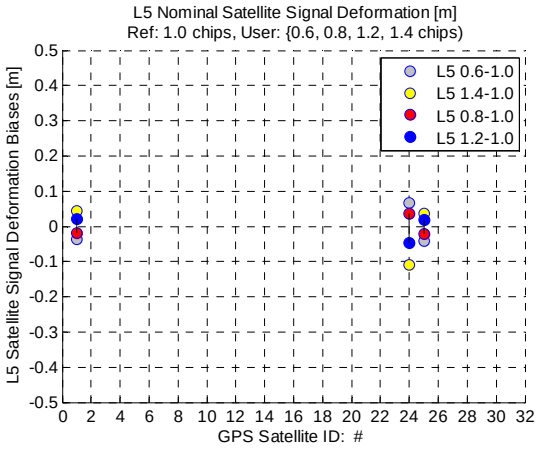

Figure 23. *Comparison of unmitigated and mitigated single-frequency L5-only signal deformation biases for all satellites.*

Similarly, as summarized in Table 11, narrowing the allowed user receiver correlator spacing reduces the maximum single-frequency L5-only bias magnitudes to 0.05 m from ~0.11 m. Similarly, the average magnitudes are also reduced to ~ 0.03 m from ~0.07 m.

Correlator. Spacing (L5-chips)		Signal Deformation Biases [m]		
Ref.	User	Min	Max	Avg Mag.
1.0	0.6-1.4	-0.11	0.07	0.07
1.0	0.8-1.2	-0.05	0.04	0.03

Table 11. *Tabular summary of unmitigated and mitigated single-frequency **L5-only** signal deformation biases*

As before, the worst case dual-frequency combination of mitigated biases is computed for these 3 satellites and used to determine if previous projections based on 2.6 × single-frequency L1-only biases are reasonable. These computed worst case dual-frequency mitigated biases are listed in Table 12.

GPS Satellite ID	Mitigated Single-Frequency L1-Only Biases		Mitigated Single-Frequency L5-Only Biases	
	User correlator spacing (L1 Chips)		*User correlator spacing (L5 Chips)*	
	0.08	0.12	0.8	1.2
1	0.01	-0.01	-0.02	0.02
24	0.01	-0.01	0.04	-0.05
25	0.01	-0.01	-0.02	0.02
Others (min)	-0.02	-0.02	-	-
Others (max)	-0.01	0.03	-	-

Table 12. *Mitigated single-frequency signal deformation biases for satellites with signals at both L1 and L5 Frequencies*
(Reference Receiver Correlator Spacings: 0.1 L1-Chips, 1.0 L5-Chips)

Table 13 shows the minimum and maximum dual-frequency biases for these three dual-frequency satellites. The biases are computed by applying the ionosphere-free equations for all possible combinations of the biases.

GPS Satellite ID	Dual-Frequency L1/L5 Bias: $2.26*Bias_{L1} - 1.26*Bias_{L5}$	
	Minimum	Maximum
1	-0.05	0.04
24	-0.06	0.07
25	-0.05	0.05

Table 13. *Maximum and minimum mitigated dual-frequency signal deformation biases for satellites with signals at both L1 and L5 frequencies, for all possible combinations of single-frequency biases from Table 12.*

Table 13 shows maximum bias magnitudes of ~0.06-0.07 m, which is approximately 2.6 times the minimum (-0.02 m) and maximum (+0.03 m) bias magnitudes for the other satellites. The results in the table show that it is reasonable to project mitigated dual-frequency biases from mitigated single-frequency L1-only biases. However, this projection needs to be verified as more dual-frequency satellites are launched in the future.

RESULTANT EXPECTED 95% AVERAGE VERTICAL POSITION ERRORS DUE TO MITIGATED SIGNAL DEFORMATION BIASES

Figures 24 and 25 show the nominal accuracy including expected 95% vertical position errors from mitigated signal deformation biases. These results are for single-frequency L1-only and dual-frequency L1/L5 WAAS users, in the case of 2 inaccessible satellites.

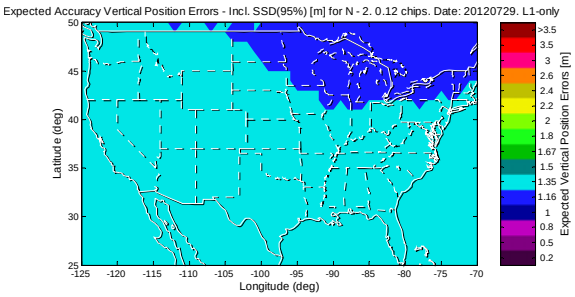

Figure 24. *Nominal Accuracy Including Expected 95% Vertical Position Errors from Mitigated Signal Deformation Biases [m] for* ***Single Frequency*** *L1-only WAAS Users, for two inaccessible satellites.*
Reference receiver: 0.1 L1-chip correlator spacing; User receiver: 0.12 L1-chip correlator spacing)

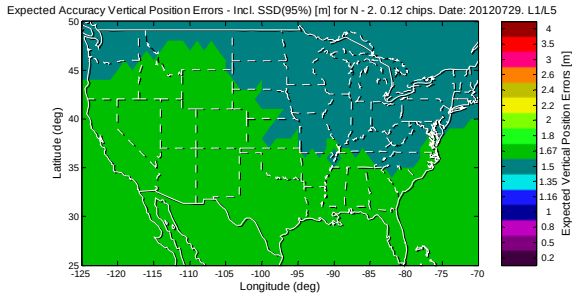

Figure 25. *Nominal Accuracy Including Expected 95% Vertical Position Errors from Mitigated Satellite Signal Deformation Biases [m] for* ***Dual Frequency*** *L1/L5 WAAS Users, for two inaccessible satellites.*
Reference receiver: 0.1 L1-chip correlator spacing; User receiver: 0.12 L1-chip correlator spacing

Tables 14 and 15 summarize the results for nominal accuracy including expected 95% vertical position errors from **mitigated** signal deformation biases, for single-frequency L1-only and dual-frequency L1/L5 users.

For single-frequency WAAS positioning, mitigated signal deformation biases contribute an additional 3% of error, compared to 16-35% for unmitigated biases. For dual-frequency WAAS positioning, the improvement is more significant: an increase of just 5%-6% (mitigated) compared to 31-76% (unmitigated) previously. These results demonstrate the benefits of signal deformation bias mitigation.

Satellite Status	Nominal Accuracy Including Expected 95% Vertical Position Errors from **Single-Frequency L1-only** Signal Deformation Biases [m]			
	User Correlator Spacing [L1-chips]			
	No SSD	Unmitigated		**Mitigated**
	0.10	**0.20**	**1.00**	**0.12**
N - 0	0.99	1.15 (+0.16) (+16.2%)	1.29 (+0.30) (+30.3%)	1.02 (+0.03) (+3.0%)
N - 1	1.07	1.24 (+0.17) (+15.9%)	1.41 (+0.34) (+31.8%)	1.10 (+0.03) (+2.8%)
N - 2	1.16	1.36 (+0.20) (+17.2%)	1.55 (+0.39) (+33.6%)	1.20 (+0.04) (+3.4%)
N - 3	1.27	1.49 (+0.22) (+17.3%)	1.71 (+0.44) (+34.6%)	1.31 (+0.04) (+3.1%)
N - 4	1.39	1.63 (+0.24) (+17.3%)	1.87 (+0.48) (+34.5%)	1.43 (+0.04) (+2.9%)
N - 5	1.50	1.76 (+0.26) (+17.3%)	2.02 (+0.52) (+34.7%)	1.55 (+0.05) (+3.3%)

Table 14. *Nominal Accuracy Including Average Expected 95% Vertical Position Errors [m] from mitigated signal deformation biases for* ***Single frequency L1-only*** *WAAS Users.*
Each row contains results for a different number of inaccessible satellites, from fully accessible to 5 inaccessible.
Vertical position errors due to unmitigated signal deformation biases are also listed for comparison.

Satellite Status	Nominal Accuracy Including Expected 95% Vertical Position Errors from **Dual-Frequency L1/L5** Signal Deformation Biases [m]			
	User Correlator Spacing [L1-chips]			
	No SSD	Unmitigated		**Mitigated**
	0.10	**0.20**	**1.00**	**0.12**
N - 0	1.21	1.59 (+0.38) (+31.4%)	1.98 (+0.77) (+63.6%)	1.27 (+0.06) (+5.0%)
N - 1	1.31	1.74 (+0.43) (+32.8%)	2.18 (+0.87) (+66.4%)	1.38 (+0.07) (+5.3%)
N - 2	1.43	1.93 (+0.50) (+35.0%)	2.43 (+1.00) (+69.9%)	1.52 (+0.09) (+6.3%)
N - 3	1.61	2.17 (+0.56) (+34.8%)	2.78 (+1.17) (+72.7%)	1.70 (+0.09) (+5.6%)
N - 4	1.82	2.48 (+0.66) (+36.3%)	3.20 (+1.38) (+75.8%)	1.93 (+0.11) (+6.0%)
N - 5	2.06	2.81 (+0.75) (+36.4%)	3.62 (+1.56) (+75.7%)	2.19 (+0.13) (+6.3%)

Table 15. *Nominal Accuracy Including Average Expected 95% Vertical Position Errors [m] from mitigated signal deformation biases for **Dual frequency L1/L5** WAAS Users.*
Each row contains results for a different number of inaccessible satellites, from fully available to 5 inaccessible.
Vertical position errors due to unmitigated signal deformation biases are also listed for comparison.

RESULTANT WORST CASE VERTICAL POSITION ERRORS DUE TO MITIGATED SIGNAL DEFORMATION BIASES

Figures 26 and 27 show the nominal accuracy including worst case vertical position errors from **mitigated** signal deformation biases. As before, these results are for single-frequency L1-only and dual-frequency L1/L5 WAAS users, for 2 inaccessible satellites.

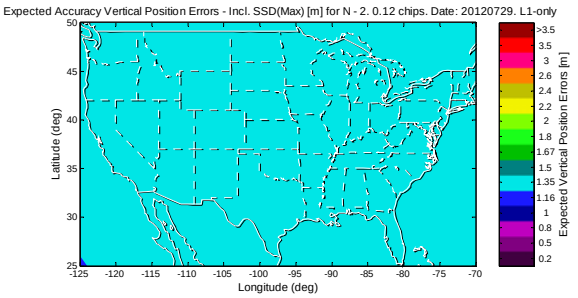

Figure 26. *Nominal Accuracy Including Worst Case Vertical Position Errors from Mitigated Signal Deformation Biases [m] for **Single Frequency** L1-only WAAS Users, for two inaccessible satellites.*
Reference receiver: 0.1 L1-chip correlator spacing; User receiver: 0.12 L1-chip correlator spacing

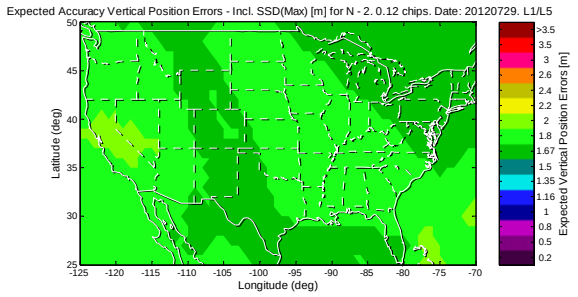

Figure 27. *Nominal Accuracy Including Worst Case Vertical Position Errors from Mitigated Satellite Signal Deformation Biases [m] for **Dual Frequency** L1/L5 WAAS Users, for two inaccessible satellites.*
Reference receiver: 0.1 L1-chip correlator spacing; User receiver: 0.12 L1-chip correlator spacing

Tables 16 and 17 summarize the results for nominal accuracy including worst case vertical position errors from mitigated signal deformation biases, for single-frequency L1-only and dual-frequency L1/L5 users.

For single-frequency L1-only WAAS positioning, the mitigated signal deformation biases now contribute an additional 4%-8% error, compared to 21-91% previously. For dual-frequency L1/L5 WAAS positioning, the mitigated biases now contribute an additional error of 7%-22%, from 44%-264% previously. These results demonstrate the effectiveness of the mitigation.

Satellite Status	Nominal Accuracy Including Worst-Case Vertical Position Errors from **Single-Frequency L1-only** Signal Deformation Biases [m]			
	User Correlator Spacing [L1-chips]			
	No SSD	Unmitigated		**Mitigated**
	0.10	**0.20**	**1.00**	**0.12**
N - 0	0.99	1.20 (+0.21) (+21.2%)	1.41 (+0.42) (42.4%)	1.03 (+0.04) (+4.0%)
N - 1	1.07	1.39 (+0.32) (+29.9%)	1.78 (+0.71) (66.4%)	1.13 (+0.06) (+5.6%)
N - 2	1.16	1.62 (+0.46) (+39.7%)	2.18 (+1.02) (87.9%)	1.24 (+0.08) (+6.9%)
N - 3	1.27	1.81 (+0.54) (+42.5%)	2.43 (+1.16) (91.3%)	1.37 (+0.10) (+7.9%)
N - 4	1.39	1.96 (+0.57) (+41.0%)	2.59 (+1.20) (86.3%)	1.49 (+0.10) (+7.2%)
N - 5	1.50	2.10 (+0.60) (+40.0%)	2.72 (+1.22) (81.3%)	1.61 (+0.11) (+7.3%)

Table 16. *Nominal Accuracy Including Worst Case Vertical Position Errors [m] from mitigated signal deformation biases for* ***Single frequency L1-only*** *WAAS Users.*
Each row contains results for a different number of inaccessible satellites, from fully available to 5 inaccessible.
Vertical position errors due to unmitigated signal deformation biases are also listed for comparison.

Satellite Status	Nominal Accuracy Including Worst-Case Vertical Position Errors from **Dual-Frequency L1/L5** Signal Deformation Biases [m]			
	User Correlator Spacing [L1-chips]			
	No SSD	Unmitigated		**Mitigated**
	0.10	**0.20**	**1.00**	**0.12**
N - 0	1.21	1.74 (+0.53) (+43.8%)	2.25 (+1.04) (+86.0%)	1.30 (+0.09) (+7.4%)
N - 1	1.31	2.24 (+0.93) (+71.0%)	3.25 (+1.94) (+148.1%)	1.47 (+0.16) (+12.2%)
N - 2	1.43	3.04 (+1.61) (+112.6%)	5.06 (+3.63) (+253.8%)	1.70 (+0.27) (+18.9%)
N - 3	1.61	3.8 (+2.19) (+136.0%)	5.86 (+4.25) (+264.0%)	1.97 (+0.36) (+22.4%)
N - 4	1.82	4.22 (+2.40) (+131.9%)	6.40 (+4.58) (+251.6%)	2.22 (+0.40) (+22.0%)
N - 5	2.06	4.48 (+2.42) (+117.5%)	6.77 (+4.71) (+228.6%)	2.46 (+0.40) (+19.4%)

Table 17. *Nominal Accuracy Including Worst Case Vertical Position Errors [m] from mitigated signal deformation biases for* ***Dual frequency L1/L5*** *WAAS Users.*
Each row contains results for a different number of inaccessible satellites, from fully available to 5 inaccessible.
Vertical position errors due to unmitigated signal deformation biases are also listed for comparison.

CONCLUSION

In this paper, the "measure-and-verify" measurement technique for L1 signal deformation biases was briefly introduced. It was subsequently extended to measurement of L5 signal deformation biases for 3 satellites transmitting dual-frequency L1/L5 signals.

These measured biases showed that it was possible and reasonable to project dual-frequency L1/L5 biases from single-frequency L1-only biases scaled by the dual-frequency ionosphere-error- removal scale factor of 2.6. This projection needs to be re-visited and verified as more dual-frequency satellites are launched.

Using the signal deformation bias measurements, the resultant vertical position errors (95% and worst case) are computed for single-frequency L1-only and dual-frequency L1/L5 WAAS users, and summarized in Tables 18 and 19.

Type of WAAS Positioning	% Increase in Expected 95% Vertical Position Errors due to Signal Deformation Biases	
	Unmitigated Biases	Mitigated Biases
Single-Frequency L1-only WAAS	16%-35%	3%
Dual-Frequency L1/L5 WAAS	31%-76%	5%-6%

Table 18. *Summary of degradation in WAAS expected 95% vertical position errors, in the presence of unmitigated and mitigated biases.*

Type of WAAS Positioning	% Increase in Worst Case Vertical Position Errors due to Signal Deformation Biases	
	Unmitigated Biases	Mitigated Biases
Single-Frequency L1-only WAAS	21%-91%	5%-6%
Dual-Frequency L1/L5 WAAS	44%-264%	7%-22%

Table 19. *Summary of degradation in WAAS worst case vertical position errors, in the presence of unmitigated and mitigated biases.*

As summarized in Tables 18 and 19, WAAS performance shows substantial degradation when unmitigated biases are present. However, restricting the allowed space of user receiver correlator spacings can substantially mitigate the adverse impact, by up to an order of magnitude. Use of this strategy would allow dual-frequency WAAS users to reap the performance benefits of dual-frequency positioning without experiencing significant degradation and limitation caused by signal deformation biases.

ACKNOWLEDGEMENT

The author would like to thank Professor Per Enge, Dr Todd Walter and Dr Eric Phelts for providing guidance and sharing their expertise and experience on the impact of signal deformation biases on WAAS. The author would also like to thank Dr Yu-Hsuan Chen for providing the USRP software receiver, without which this research would have been very difficult. Finally, the author would also like to thank Professor Dennis Akos for sharing his expertise on software receivers, regular antennas, beam-forming antennas and signal deformation bias measurements.

In addition, the author is grateful to the Federal Aviation Administration for their continuing generous sponsorship of this research.

REFERENCES

[1] Brenner, M., Kline, P., Reuter, R., "Performance of a Prototype Local Area Augmentation System (LAAS) Ground Installation", Proceedings of ION GPS 2002, Portland, OR, Sep 2002

[2] Blanch, J., Walter, T., Enge, P., "A Clock and Ephemeris Algorithm for Dual Frequency SBAS", Proceedings of the 24th International Technical Meeting of The Satellite Division of the Institute of Navigation (ION GNSS 2011), Portland, September 2011

[3] Chen, Y-H., Juang, J-C., et. al, "Real-Time Software Receiver for GPS Controlled Reception Pattern Array Processing", Proceedings of the 23rd International Technical Meeting of The Satellite Division of the Institute of Navigation (ION GNSS 2010)

[4] Chen, Y-H., "A Study of Geometry and Commercial Off-The-Shelf (COTS) Antennas for Controlled Reception Pattern Antenna (CRPA) Arrays", Proceedings of the 25th International Technical Meeting of The Satellite Division of the Institute of Navigation (ION GNSS 2012), Nashville, September 2012

[5] Chen, Y-H., Juang, J-C., et al, "Design and Implementation of Real-time a Software Radio for Anti-Interference GPS/WAAS Sensors", Accepted for Publication Sensors 2012

[6] Gunawardeena, S., van Grass, F., "Analysis of GPS Pseudorange Natural Biases using a Software Receiver", Proceedings of the 25th International Technical Meeting of The Satellite Division of the Institute of Navigation (ION GNSS 2012), Nashville, September 2012

[7] Jan, S., Chan, W., Walter, T., and Enge, P., "Matlab Simulation Toolset for SBAS Availability Analysis", Proceedings of the 14th International Technical Meeting of the Satellite Division of The Institute of Navigation (ION GPS 2001), Salt Lake City, September 2001

[8] Phelts, R.E., "Nominal Signal Deformations: Limits on GPS Range Accuracy", The 2004 International Symposium on GPS/GNSS, Sydney, Australia, December 2004

[9] Phelts, R. E., Walter, T., Enge, P., "Characterizing Nominal Analog Signal Deformations on GNSS Signals", Proceedings of the 22nd International Technical Meeting of The Satellite Division of the Institute of Navigation (ION GNSS 2009), Savannah, GA, September 2009

[10] Walter, Todd, Enge, Per, Hansen, Andrew, "A Proposed Integrity Equation for WAAS MOPS", Proceedings of the 10th International Technical Meeting

of the Satellite Division of The Institute of Navigation (ION GPS 1997), Kansas City, MO, September 1997, pp. 475-484.

[11] Walter, T., Blanch, J., Enge, P., "Vertical Protection Level Equations for Dual Frequency SBAS", Proceedings of the 23rd International Technical Meeting of The Satellite Division of the Institute of Navigation (ION GNSS 2010), Portland, OR, September 2010, pp. 2031-2041

[12] Wong, G., Phelts, R.E., Walter, T., Enge, P., "Characterization of Signal Deformations for GPS and WAAS Satellites", Proceedings of the 23rd International Technical Meeting of The Satellite Division of the Institute of Navigation (ION GNSS 2010), Portland, September 2010

[13] Wong, G., Phelts, R.E., Walter, T., Enge, P., "Alternative Characterization of Analog Signal Deformation for GNSS-GPS Satellites", Proceedings of the 2011 International Technical Meeting of The Institute of Navigation, San Diego, January 2011

[14] Wong, G., Phelts, R.E., Walter, T., Enge, P., "Bounding Errors Caused by Nominal GNSS Signal Deformations", Proceedings of the 24th International Technical Meeting of The Satellite Division of the Institute of Navigation (ION GNSS 2011), Portland, September 2011

[15] Wong, G., Chen, Y-H., Phelts, R.E., Walter, T., Enge, P., "Measuring Code-Phase Differences due to Inter-Satellite Hardware Differences", Proceedings of the 25th International Technical Meeting of The Satellite Division of the Institute of Navigation (ION GNSS 2012), Nashville, September 2012

[16] Federal Aviation Administration website, "Wide Area Augmentation System", http://www.faa.gov/ about/office_org/headquarters_offices/ato/service_units/techops/navservices/gnss/waas/

[17] Lancaster University Department of Physics website, "Glossary of Terms", http://spears.lancs.ac.uk/ glossary/